

Structure, magnetization and Mössbauer study of nanostructured $\text{Ni}_{0.5}\text{Zn}_{0.5}\text{Fe}_2\text{O}_4$ ferrite powders

Shihui Ge¹, Zongtao Zhang¹, Mingzhong Wu¹, Y.D. Zhang¹, D. P. Yang², J. I. Budnick³,
and W. A. Hines³

¹Inframat Corporation, 74 Batterson Park Road, Farmington, CT 06032

²Physics Department, College of the Holy Cross, Worcester, MA 01610

³Department of Physics and Institute of Materials Science, University of Connecticut, Storrs, CT 06269

ABSTRACT

Nanostructured ferrites possess more advantages than the conventional ferrite materials and have been a research focus recently. In this work, a series of nanostructured $\text{Ni}_{0.5}\text{Zn}_{0.5}\text{Fe}_2\text{O}_4$ were synthesized by a citrate reaction method followed by calcining at various temperatures with the goal of obtaining pure phase $\text{Ni}_{0.5}\text{Zn}_{0.5}\text{Fe}_2\text{O}_4$ nanoparticle while keeping the size small. X-ray diffraction, transmission electron microscopy, SQUID magnetometry and Mössbauer spectroscopy (ME) have been employed to characterize the crystal structure, phase homogeneity, particle size, the conditions for reaction completion, and the magnetic properties. The results show that the saturation magnetization M_s at both 10K and 300K increase with increasing calcination temperature T_{ca} , but particle size also increases with T_{ca} . Three factors, the incomplete reaction for ferrite phase formation, the surface effect and superparamagnetic behavior, are found to be responsible for low M_s values at lower T_{ca} . Based on a detailed analysis of nanostructure and magnetic properties in ferrites, the optimal conditions for synthesizing nanostructured $\text{Ni}_{0.5}\text{Zn}_{0.5}\text{Fe}_2\text{O}_4$ have been established.

INTRODUCTION

Ferrites have been used as high frequency soft magnetic materials for several decades due to its high resistivity and higher permeability [1]. Nanostructured ferrites possess some fundamental advantages over the conventional ferrite materials, such as the possibility to develop high density magnetic storage media with nanosized constituent particles or crystallites [2], the combination with a large variety of immiscible insulating or metallic particles on nanoscale to form new nanocomposites [3], and so on, which makes the nanostructured ferrites become a research focus recently. Various novel approaches such as chemical co-precipitation [4], the sol-gel method [5], hydrothermal processing [6], high energy ball milling [7], pulse-laser deposition [8], sputter deposition [9], and spin-spray plating [10], have been employed to produce nanoparticles and thin film ferrite materials. A common problem occurs when characterizing the structural and magnetic properties. That is, the saturation magnetization of the ferrite particles decreases when we reduce the particle size, which is not favored in applications. In order to elucidate the origin of this reduction of saturation magnetization and look for the optimal conditions for synthesizing nanostructured $\text{Ni}_{0.5}\text{Zn}_{0.5}\text{Fe}_2\text{O}_4$, a series of $\text{Ni}_{0.5}\text{Zn}_{0.5}\text{Fe}_2\text{O}_4$ ferrite powders have been synthesized using a wet chemistry method followed by calcining at various temperatures, and a systematic structural and magnetic property analysis was carried out in this work via a combined study of X-ray diffraction, SQUID magnetometry and Mössbauer spectroscopy. Based on the experimental results and analysis, the optimum processing parameters for $\text{Ni}_{0.5}\text{Zn}_{0.5}\text{Fe}_2\text{O}_4$ nanoparticles have been obtained.

EXPERIMENTAL

Nanostructured $\text{Ni}_{0.5}\text{Zn}_{0.5}\text{Fe}_2\text{O}_4$ ferrites were synthesized by a low-temperature approach based on the sol-gel auto-combustion method [11]. Appropriate amounts of nickel nitrate, zinc nitrate, and iron (III) citrate were dissolved in deionized (DI) water. Citric acid was added as a gelating agent. The solution was mixed and slowly dried until the solution was concentrated. The mixture was further dried in an oven at 40°C for 12 hours, resulting in porous agglomerate (precursor). A series of Ni-Zn ferrite powder samples were obtained by calcining the precursor in controlled oxygen atmosphere at different temperatures for three hours.

The phase, structure and particle size of the synthesized powders were characterized by X-ray diffraction (XRD) with $\text{Cu K}\alpha_1$ radiation and high-resolution transmission electron microscopy (HRTEM). Mössbauer spectra were obtained with a constant-acceleration Mössbauer spectrometer at various temperatures between 20 K and 300 K. The static magnetic properties of synthesized $\text{Ni}_{0.5}\text{Zn}_{0.5}\text{Fe}_2\text{O}_4$ particles were measured using a Quantum Design SQUID magnetometer at temperatures between 10 K and 300 K.

RESULTS AND DISCUSSION

Figure 1 shows the XRD patterns of $\text{Ni}_{0.5}\text{Zn}_{0.5}\text{Fe}_2\text{O}_4$ powder samples calcined at various temperatures. For comparison, the figure also includes the XRD patterns of precursor and a conventional (with bulk-size) $\text{Ni}_{0.5}\text{Zn}_{0.5}\text{Fe}_2\text{O}_4$ powder. The XRD results identify that all samples have the same cubic spinel structure of Ni-Zn ferrite, while the precursor does not exhibit diffraction peak and therefore is amorphous. The linewidths of the diffraction peaks for nanostructured $\text{Ni}_{0.5}\text{Zn}_{0.5}\text{Fe}_2\text{O}_4$ are significantly broader than that of the bulk material. From the linewidth of the main peak (at $2\theta = 35.6^\circ$), the mean grain size was calculated following the Scherrer equation [12]. Figure 2 shows the grain size D of synthesized $\text{Ni}_{0.5}\text{Zn}_{0.5}\text{Fe}_2\text{O}_4$ powders as a function of calcination temperature T_{ca} . It can be seen that D increases with increasing calcination temperature, and the grain size is less than 22 nm below 650°C .

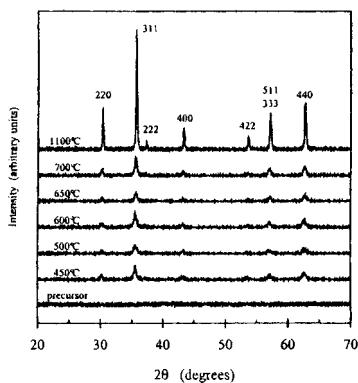


Figure 1. X-ray diffraction patterns of the precursor and calcined samples of nanoparticle $(\text{Ni}_{0.5}\text{Zn}_{0.5})\text{Fe}_2\text{O}_4$, obtained using $\text{Cu K}\alpha$ radiation.

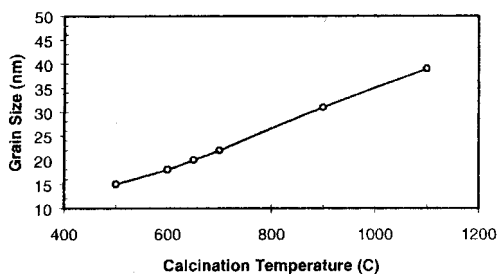


Figure 2. Grain size D of synthesized $\text{Ni}_{0.5}\text{Zn}_{0.5}\text{Fe}_2\text{O}_4$ powders as a function of calcination temperature T_{ca} .

Figure 3 depicts the typical magnetization curve measured at 10 K and 300 K for the sample calcined at 500°C. To simplify the analysis, the magnetization values under 55 kOe at 10 K were taken as the saturation magnetization M_s for all samples. For comparison, the saturation magnetization of bulk $\text{Ni}_{10.5}\text{Zn}_{0.5}\text{Fe}_2\text{O}_4$, $4\pi M_s = 8867\text{Gs}$, reported by literature [1], was taken as the expected saturation magnetization. Figure 4 shows M_s as a function of calcination temperature, where M_s increases with increasing T_{ca} , but the curve has a lower slope when T_{ca} is higher than 650°C. In order to control both the grain size and M_s more efficiently, an investigation into the origins of the reduced M_s for the samples with smaller grain sizes is necessary.

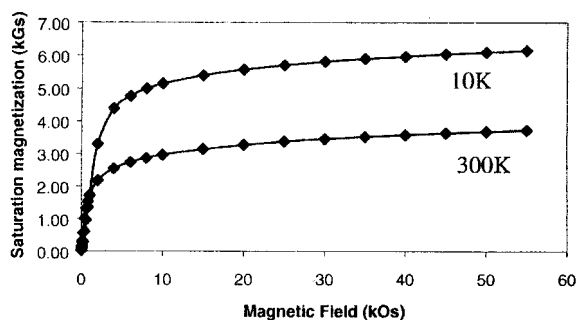


Fig.3 magnetization curve measured at 10 K and 300K for the sample calcined at 500°C

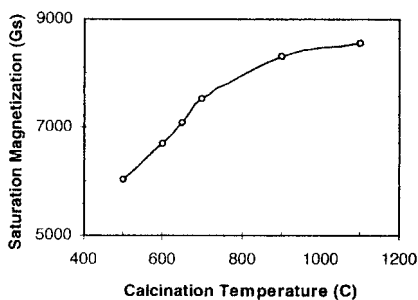


Figure 4. Saturation magnetization as a function of calcination temperature

Three factors are possibly responsible for the low M_s values for samples calcined at low temperatures. First, the reaction for forming $\text{Ni}_{10.5}\text{Zn}_{0.5}\text{Fe}_2\text{O}_4$ may not be completed

under the low-temperature calcination condition, which has been confirmed by a Mössbauer effect study. Figure 5 shows the room-temperature Mössbauer spectra for samples calcined at different temperatures [13]. The spectrum of the precursor consists of solely a quadruple doublet, indicating the paramagnetic nature of Fe atoms in the precursor. The spectra of the samples calcined below 650°C exhibit a broad sextet and a doublet. The former is identified to be the Ni-ZnFe₂O₄ phase while the latter is from the remaining precursor, indicating incomplete reaction at these calcination temperatures. Since the precursor has no magnetization, these incompletely reacted samples possess smaller saturation magnetization. When T_{ca} is higher than 650°C, the spectrum is composed essentially of pure magnetic sextets, indicating that 650°C is the threshold of calcining temperature for a complete reaction for ferrite phase formation.

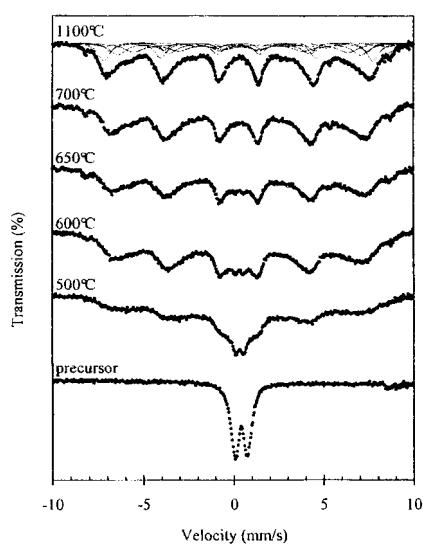


Figure 5. Room-temperature ⁵⁷Fe Mössbauer spectra of nanoparticle (Ni_{0.5}Zn_{0.5})Fe₂O₄ samples calcined at various temperatures

Second, the surface region of a nanoparticle may be in a spin-disordered state, which leads to a further reduction of saturation magnetization. It is well known that the unequal sublattice magnetization gives rise to ferrimagnetism. For ferrite, the saturation magnetization comes from the difference of the magnetizations of the magnetic cations in the two sublattices (one is tetrahedral, and another is octahedral). The magnetic moments of these cations are coupled by superexchange interaction through oxygen ions between them. Since the intersublattice exchange interaction (negative) is stronger than the intrasublattice exchange (positive), the magnetizations of the two sublattices are antiparallel, thus leading to a net uncompensated magnetization if the magnetizations of the two sublattices are not equal. The exchange bonds may be broken if an oxygen ion is

missing on the surface. For the cations in the surface region, the loss of surrounding symmetry and the reduction of coordination result in a frustration of the superexchange interaction such that these cations experience less and inhomogeneous interaction than those in the interior. This leads to a reduction of the magnetization of the surface region [2]. The smaller the particle size, the larger the relative amount of surface atoms involved in disordering and, consequently, the larger the reduction of magnetization. As shown in Fig. 5, Mössbauer spectra for the samples calcined at lower temperatures exhibit a large linewidth, about 0.5 mm/s. This inhomogeneous hyperfine field distribution is consistent with the Fe spin disorder. Furthermore, since the surface cations are less controlled by the superexchange interaction, they behave more like paramagnetic. This is observed in the magnetizations curves shown in Fig. 3: the magnetization curves contain a large contribution from paramagnetic cations in high field magnetization process and are not saturated up to 5.5 T.

Third, superparamagnetic relaxation exists in samples calcined at lower temperatures due to the small particle size, which leads a significant reduction of the room temperature saturation magnetization as shown in Fig. 3. Figure 6 shows the magnetic hysteresis loops at both 300 K and 10 K. The loop at 300 K exhibits very small hysteresis behavior, namely, H_c and M_r are both close to zero, implying that most of particles are superparamagnetism. This superparamagnetic behavior has also been evidenced by a low-temperature Mössbauer experiment study where the intensity of magnetic sextet subspectrum at 20 K increases significantly in comparison with that of room-temperature spectrum for the sample calcined at 500°C.

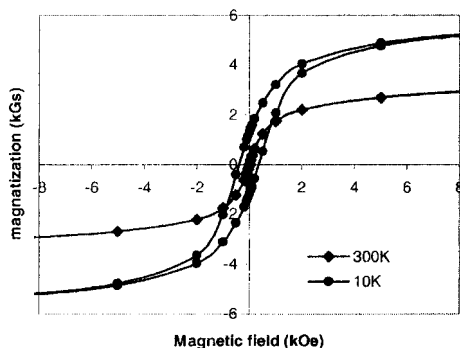


Figure 6. Magnetic hysteresis loops measured at 300 K and 10 K for the sample calcined at 500°C.

Comparing the influence of the three factors on the magnetic properties, the surface spin disorder and the superparamagnetic relaxation can not be avoided for small particles, but the complete reaction can be obtained by optimizing the calcination temperature. Based on our study, the calcining at 650-700°C is recommended.

CONCLUSIONS

Nanosized $\text{Ni}_{0.5}\text{Zn}_{0.5}\text{Fe}_2\text{O}_4$ have been synthesized by a modified sol-gel method. By adjusting the calcinations temperature, a pure $\text{Ni}_{0.5}\text{Zn}_{0.5}\text{Fe}_2\text{O}_4$ phase can be obtained, and the grain size can be controlled. The optimal calcination temperature is between 650 and 700°C, which leads to a saturation magnetization of 7086 Gs and a grain size of 21 nm. Such $\text{Ni}_{0.5}\text{Zn}_{0.5}\text{Fe}_2\text{O}_4$ nanopowder will be a good candidate for fabrication of nanophase $\text{Ni}_{0.5}\text{Zn}_{0.5}\text{Fe}_2\text{O}_4$ material for high-frequency applications.

Acknowledgments: Work supported by DARPA Contract No. F7-6AM945-X05 and the Space Directorate of the Air Force Research Laboratory and the Air Force Small Business Innovative Research program Contract No. F29601-02-C-0031.

REFERENCES

1. Smit and H. P. J. Wijn, *Ferrites*, (Philips', Holland, 1959).
2. R.H. Kodama, A. E. Berkowitz, E. J. McNiff, Jr. and S. Foner, *Phys. Rev. Lett.*, **77** (1996) 394.
3. Adriana S. Albuquerque, Jose D. Ardisson, Waldemar A.A. Macedo, J. Magn. Mater. **192** (1999) 277.
4. H. Tang, Y. W. Du, Z. Q. Qiu, and J. C. Walker, *J. Appl. Phys.* **63**, 4105 (1988).
5. L. L. Hench and J. K. West, *Chem. Rev.* **90**, 33 (1990).
6. A. Dias, N. D. S. Mohallem, and R. L. Moreira, *J. de Phys.* III **6**, 843 (1996).
7. J. S. Jiang, L. Gao, X. L. Yang, J. K. Guo, and H. L. Shen, *J. Mater. Sci. Lett.* **18**, 1781 (1999).
8. F. W. Oliver, D. Seifu, E. Hoffman, D. B. Chrisey, J. S. Horwitz, and P. C. Dorsey, *Appl. Phys. Lett.* **75**, 2993 (1999).
9. M. Desai, S. Prasad, N. Venkataramani, I. Samajdar, A. K. Nigam, N. Keller, R. Krishnan, E. M. Baggio-Saitovitch, B.R., Pujada, and A. Rossi, *J. Appl. Phys.* **91**, 7592 (2002).
10. N. Matsushita, C. P. Chong, T. Mizutani, and M. Abe, *J. Appl. Phys.* **91**, 7376 (2002).
11. A. Verma, T. C. Goel, and R. G. Mendiratta, *Mater. Sci. Technol.*, **16**, 712 (2000).
12. H. Lipson and H. Steeple, *Interpretation of X-ray powder Diffraction Patterns* (St Martin's Press, New York, 1970) p. 256.
13. De-Ping Yang, Lindsey K. Lavoie, Yide Zhang, Zhongtao Zhang and Shihui Ge, to be published in *J. Appl. Phys.*